X-611-68-108

THE INTENSITY AND TIME VARIATION OF PRIMARY COSMIC RAY ELECTRONS

G. M. Simnett

March 1968

Goddard Space Flight Center
Greenbelt, Maryland

THE INTENSITY AND TIME VARIATION OF PRIMARY COSMIC RAY ELECTRONS

G. M. Simnett

March 1968

Goddard Space Flight Center
Greenbelt, Maryland

ABSTRACT

The primary cosmic ray electron differential energy spectrum between 30 MeV and 1500 MeV has been measured with a system composed of a Cerenkov telescope and a lead-scintillator sandwich detector. Results are presented from a balloon flight made at Kiruna, Northern Sweden, in 1967, and these are compared with measurements made in 1965 with a similar detector. The results are well represented by a power law spectrum of the form:

$$\frac{dJ}{dE} = 14^{+2}_{-3}\ E^{-0.7 \pm 0.1}\ \text{electrons/m}^2\ \text{sec, so MeV}$$

between 150 MeV and 800 MeV. There is evidence for a rigidity independent (solar) modulation of the electron flux below 600 MeV, which is the highest energy where the results are comparable. The lower limit to the modulation is 20%. There is no evidence for a diurnal variation in the electron intensity.

The results of other comparable balloon borne electron experiments are discussed.

THE INTENSITY AND TIME VARIATION OF PRIMARY COSMIC RAY ELECTRONS

The electronic component of the cosmic radiation is a useful tool for the investigation of certain galactic properties, which should eventually lead to significant improvements in our knowledge of cosmic ray sources and how cosmic rays propagate through the interstellar medium. Radio astronomical studies can establish crudely the shape of the source electron spectrum and thickness of the radiating region, together with its intensity as a function of magnetic field. Subsequently on their passage through interstellar space the electrons undergo energy changes through ionization, Compton, knock-on and synchrotron processes, and intensity changes largely through the injection of muon decay products. Muon decay electrons and positions also alter the change ratio and spectrum of the total electron flux. Below energies of 1 - 2 GeV the electronic component can be used to study solar modulation of cosmic rays. The high charge/mass ratio of the electron is unique, and it is particularly informative to study relative changes of the electronic and nucleonic components of cosmic rays.

Synchrotron radiation from high energy electrons moving in a magnetic field prompted the first successful attempts in 1960 to isolate and measure the electronic component of the cosmic ray beam incident at the Earth (Meyer & Vogt, 1961; Earl, 1961). Since 1960 techniques have improved and data have accumulated to reveal the differential energy spectrum and charge ratio of primary electrons (Cline, Ludwig and McDonald, 1964; Schmoker and Earl, 1965; L'Heureux and Meyer, 1965; Freier and Waddington, 1965; Bland, Boella, Degli Antoni, Dilworth, Scarsi, Sironi, Agrinier, Koechlin, Parlier and Vasseur, 1966; Daniel and Stephens 1965, 1966, Rubtsov, 1966, L'Heureux, 1967, L'Heureux and Meyer, 1967; Beedle and Webber, 1967; Webber and Chotkowski, 1967, Bleeker, Burger, Deerenberg, Scheepmaker, Swanenburg and Tanaka, 1967; Simnett, 1967; Fanselow, 1967; Danjo, Hayakawa, Makino and Tanaka, 1967). Most reported measurements have been from balloon flights of duration typically less than one day at altitudes of several g cm $^{-2}$ of residual atmosphere. The results are susceptible to intensity changes of the primary flux, probably associated with solar activity, and to correction for atmospheric secondary electrons.

Currently there is no evidence that the galactic electron flux is variable and it is assumed that all primary intensity changes are solar induced. The contribution of solar accelerated electrons to the total intensity is still uncertain, but solar densities and magnetic fields make it unlikely that during "quiet" times electrons of more than a few MeV are emitted from the Sun.

We report here the results of a balloon flight made in 1967 to detect electrons in the energy range 20 MeV to 1500 MeV and we compare these with the results from flights made with a similar detector in 1965. The diurnal variation is discussed and it is shown that the data are consistent with a solar modulation of the primary electron intensity. Where relevant the differences between the detectors flown in 1965 and 1967 are indicated, although overall absorber thicknesses were kept constant between the two detectors in the interest of studying the effect of solar modulation.

The Experimental Details

The electron detector flown in 1967 is an improved version of that flown in 1965, and a schematic cross section of the detector is shown in Figure 1. Relativistic charged particles with a lower velocity threshold corresponding to $\beta = 0.78$ are selected by a three element coincidence telescope. The uppermost element of the telescope is a plastic scintillator of NE102A, and the lowest telescope element is a liquid Cerenkov detector which uses FC75* (refractive index 1.274 at 25°C) as the radiating medium. This latter element sets the lower velocity threshold of the telescope, and between them these elements define the acceptance cone for incident particles. The geometric factor is 9.8 ± 0.5 cm^2 sr. An inclined element of Perspex, blackened over its upper surface, is used as the middle element of the telescope, and this rejects approximately 85% of upward moving particles. This compares unfavorably with the rejection efficiency of >98% of upward moving particles for the detector flown in 1965. However, the variation with incident angle of the thickness of the telescope in g cm^{-2} is an order of magnitude lower than in the 1965 detector, which contained a 5" photomultiplier tube inside the acceptance cone. This leads to a more uniform response to electrons as a function of incident direction.

---

*Supplied by the Minnesota Mining and Manufacturing Company

Electron identification and energy measurement is achieved with a lead-scintillator sandwich detector which consists of three lead blocks, of thickness 2, 3 and 6 radiation lengths respectively, each followed by a plastic scintillator detector of NE102A. These scintillators are referred to as S_1, S_2 and S_3. S_1 is used to detect electrons which are absorbed in the first 2 radiation lengths of lead, and a 16 channel pulse height analysis is performed on the outputs of S_2 and S_3. The term "electron" in this context is used to describe the incident electron plus its progeny. No distinction is made between electrons and positions. Electron events are recognized by a telescope coincidence which is unaccompanied by a pulse from S_3. Electron events which penetrate S_3 are in general not recognized unambiguously from relativistic alpha particles. However, electrons which have been reduced to one shower particle on emergence from the lead absorber can be identified and this information is used to extend the upper energy limit to 1500 MeV. The two-dimensional pulse height analysis also serves as an in-flight check of the calibration of the detector. An artificially accelerated electron beam from DESY, Hamburg, was used to determine the overall response of the detector between 50 MeV and 3 GeV.

S_1, S_2 and S_3 extend outside the solid angle defined by the Cerenkov telescope to minimize the effect of proton-nucleon scattering in the absorber. It is not advantageous to extend such a guard beyond a certain limit, as the majority of particles which emerge from the lead at large angles to the telescope axis are electrons. We extended the scintillators to cover a possible scattering angle of 20-25° outside the most oblique direction defined by the telescope.

The correction to be applied to the electron counting rates from other cosmic ray components has been calculated. The proton spectrum used is that given by Ormes and Webber (1964). The correction for proton interactions in the lead absorber includes the contribution from protons which are scattered outside the scintillator guard. The correction for upward moving particles produced in the absorber by protons entering from the side, neutrons and gamma rays, is based on a measurement of such particles made by the 1965 detector (Simnett, 1966). This is referred to as the neutron and gamma ray correction. The detailed detector response to protons, alpha particles, mesons, gamma rays and nuclei with $Z > 2$ has been analysed in detail elsewhere (Simnett 1966). The corrections are summarized in Table I. Included in Table I is the percentage of the correction applied to each of the electron components, which are defined in the following section. The correction for downward moving neutrons is negligible. The correction for downward moving gamma rays is of the order of $0.5/m^2$ sec. sr. and is included in the neutron and gamma ray correction.

Experimental Results

The detector was launched from Kiruna, Sweden (geomagnetic latitude $\lambda = 65.3°N$) at 21.38 U.T. on August 5th 1967. Details of the flight path are given in Table II, and it should be noted that the balloon drifted north in geomagnetic latitude throughout the flight. During its ascent phase the balloon drifted approximately 60 miles north and it reached a floating altitude of 3.7 g cm^{-2} of residual atmosphere at 23.45 U.T. A 0.1 W F.M. transmitter, operating at 137

Mc/s provided the data link from the ballon to ground. Data were received at two locations, one at Kiruna and the other at Andennes, Norway up to 14.00 U.T. on August 6th, 1967. At this time the balloon had sunk to 4.5 g cm^{-2} of residual atmosphere.

The electron data are divided into six groups, which are referred to as A, B, C, D, E and F. A and B correspond to electrons which are stopped between 0 and 2 and between 2 and 5 radiation lengths of lead respectively. Groups C, D and E correspond to electrons which are stopped between 5 and 11 radiation lengths of lead and they are distinguished according to the pulse height in S_2. C corresponds to the lowest energy in this category and E to the highest energy. Group F consists of electrons which produce a saturation pulse in S_2 and a pulse in one of the lowest five channels of the S_3 pulse height analyser. The energy at which the maximum detector response occurs is given in Table III for each group.

The electron counting rates as a function of atmospheric depth are shown in Figures 2-4 for groups A, B, and C, D, E respectively. The points are corrected for the interactions in the detector (summarized in Table I) but include atmospheric secondary electrons. The largest correction was $\approx 9\%$ at floating altitude to C. Figure 5 shows the sum of groups C, D and E, which corresponds to the total electron flux absorbed between 5 and 11 radiation lengths of lead, as a function of atmospheric depth.

One of the major problems with a balloon borne experiment is that of atmospheric secondary contamination. Recent theoretical calculations (Verma, 1966; Perola and Scarsi, 1966; Smorodin, 1965) using data from both the primary cosmic ray flux and nuclear interactions in the atmospheric disagree on the magnitude of the secondary flux, although the shape of the spectrum and the atmospheric depth dependence are not widely disputed. However, the solar minimum primary cosmic ray flux on which these calculations were based (with the exception of Smorodin) is not relevant to observations made in 1967 and there is no justification for applying rigorously the theoretical results to the present data.

A more satisfactory method of obtaining the atmospheric secondary electron correction utilizes the experimentally determined electron growth curves through the atmosphere. The term "atmospheric secondaries" does not include those electrons which are the progeny of electrons incident at the top of the atmosphere. These are accounted for in the atmospheric depth curves of primary electrons, which are discussed below.

The following considerations were made in the derivation of the atmospheric secondary electron flux.

1) At 0 g cm^{-2} of residual atmosphere the secondary electron flux is zero.
2) Below approximately 60 g cm^{-2} of residual atmosphere the contribution to the electron flux from primary, or extra-terrestrial electrons is negligible compared with the contribution from atmospheric secondary electrons.

3) Theoretical calculations (Perola and Scarsi, 1966; Verma, 1966) predict a linear growth of secondary electrons versus atmospheric depth between 2 g cm^{-2} and 10 g cm^{-2} of atmosphere.

4) Between 10 g cm^{-2} and 60 g cm^{-2} of atmosphere the secondary electron flux increases smoothly.

The results are shown in Figures 2, 3 and 5 for groups A, B and (C+D+E) respectively. The secondary derivation has been restricted to these groups on account of the poor statistical accuracy of the individual growth curves for groups C, D, E and F. The question now arises as to how the secondary flux for (C+D+E) should be divided among C, D and E. We assumed that the secondary contributions in these groups are in the ratio of the measured fluxes at 3.7 g cm^{-2}, of residual atmosphere. Physically this means that the secondary spectrum is similar in shape to the primary spectrum between approximately 450-1500 MeV. The results of Verma, (1967), Smorodin (1965) and Perola and Scarsi (1966) show that this is not unreasonable. However, as the secondary correction is approximately 20% of the measured flux for (C+D+E), the error in the primary spectrum from the use of the above approach will be small.

The differential energy spectrum of non-secondary electrons at 3.7 g cm^{-2} of residual atmosphere may now be computed from the DESY electron synchrotron calibration data and the measured flux. The results are given in Table IV and Figure 9. The atmospheric depth dependence of this spectrum plus its progeny was calculated using a Monte Carlo process. Ionization and bremsstrahlung losses were considered for electrons and pair production and the Compton effect were considered for gamma rays. Relevant cross sections were taken from Rossi (1952). The results are shown as the dashed line in Figures 2, 3 and 5. The sum of the incident electron flux plus progeny and the atmospheric secondary electron flux is also shown. It was required that this should be in good agreement with the experimental data points. Consequently an iterative procedure had to be used, which computed a crude spectrum initially and made successive corrections to the secondary flux, primary electron spectrum and its depth dependence until good agreement was reached with the experimental data points. The curves shown in Figures 2, 3 and 5, and the values in Table IV represent the final results of this procedure.

The atmospheric secondary electron spectrum may also be established from this analysis, and the result is shown in Fig. 6. The spectra proposed by Perola and Scarsi (1966) and Verma (1966) for an atmospheric depth of 4 g cm^{-2} at solar minimum are shown for comparison. The theoretical calculations are both higher than the experimental points. This has also been reported by Beedle and Webber (1967).

The Diurnal Variation of the Incident Electron Flux and Cut-Off Rigidity

One of the objectives of the present flight was to study the diurnal variation of the electron intensity. The uncorrected electron intensity is shown in Fig. 7 as a function of time for all groups. The "non-electronic" intensity is also included in Fig. 7. At the altitude of the balloon the "non-electronic" intensity is composed predominantly of protons and alpha particles. It is equivalent to the sum of the integral proton flux above approximately 900 MeV and the integral alpha particle flux above approximately 700 MeV/nucleon.

The data shown in Fig. 7 start at the time the balloon reached its floating altitude of 3.7 g cm^{-2} of residual atmosphere and end approximately 14 hours later when the balloon had fallen to 4.5 g cm^{-2}. There is a gap in the data around 0900 U.T. when the reception was poor at Kiruna and had not commenced at Andennes. There is little evidence for a genuine diurnal variation in any of the components. The largest variation was +38% in group E, which had the poorest statistical accuracy. The data were divided into those intervals of approximately 4 hours each for this analysis. The second largest variation was +25% in group B. The remaining groups were constant to within 10%. None of these results is inconsistent with statistical variations combined with changes in atmospheric depth.

It is informative to discuss the implications of this result. Throughout the flight the geomagnetic latitude of the balloon steadily increased. When the balloon reached its floating altitude 40 minutes after local midnight it was at a geomagnetic latitude of 66.1 ± 0.1°N. At this time and position the geomagnetic cut-off rigidity was likely to have been less than 45 MV (Paulikas, Blake and Freden, 1968; Stone, 1964) and probably zero (Hakura, 1967; Reid and Sauer, 1967). The reduction from the classical Störmer cut-off arises through the interaction of the solar wind with the geomagnetic field, and it is particularly noticeable at high latitudes. The average value of the Kp index throughout the balloon flight was 1 +; therefore this period may be termed magnetically quiet.

A cut-off rigidity of ≤ 45 MV means that the incident electron intensity must be predominantly, if not completely, of primary origin at the time the balloon reached its ceiling altitude. If the geomagnetic cut-off at the location of the balloon increased towards local noon, a change in intensity of the lowest energy electron component, Group A, should have been observed. This did not occur within the statistical accuracy of the measurement. It was evident from the "non electronic" intensity, which should not vary with time over the period of one day, and the detector pulse height analysis that there were no instrumental changes throughout the period of the flight. It has been suggested (Reid and Sauer, 1967; Taylor, 1967) that low rigidity interplanetary particles have access to regions of higher cut-off rigidity through longitudinal drift from points connected to the geomagnetic tail. We are thus faced with the possibility that there is only partial exclusion of low rigidity interplanetary electrons towards local noon, and that this is exactly balanced by partial inclusion of re-entrant albedo electrons of similar rigidities. An alternative explanation of the present results is that the cut-off at the location of the balloon was below the combined air plus instrument cut off (which is ≈ 30 MV for electrons) throughout the flight. Satellite results of Stone (1964) show that the cut-off latitude at local noon can be as low as 67° for 1.5 MeV (53 MV) protons during magnetically quiet periods and the fact that no diurnal variation is observed supports this explanation. It is inconceivable to go to the other extreme where the cut-off rigidity at the location of the balloon is always higher than the highest energy measured.

To summarize, it is unlikely that the electron intensity is contaminated by re-entrant albedo in the 3-4 hours following local midnight. It would be fortuitous if, towards local noon, the exclusion of primary electrons were exactly balanced by the inclusion of re-entrant albedo. There is no justification for applying a re-entrant albedo correction to the present results.

Modulation of the Electron Flux

The data from the present flight may be compared with data from a flight from Kiruna on 29th August 1965 which was made with a similar detector (Simnett 1967). Figure 8 shows the electron intensity as a function of atmospheric depth for electrons stopped between 0 and 5 radiation lengths of lead (low energy component) and between 5 and 11 radiation lengths of lead (high energy component) for both 1965 and 1967. The curves are corrected for interactions in the detectors but include atmospheric secondary electrons. The highest altitude data points, which are statistically the most significant, are lower in 1967 by 23 ± 3% (low energy component) and 24 ± 3% (high energy component). The "non electronic" intensity, which is predominantly protons and alpha particles at high altitudes, fell by 15 ± 2% over the same period. The atmospheric secondary electron correction is unlikely to change by more than 15% between 1965 and 1967 as it is produced mainly by the high energy nucleon flux (> 1 GeV).

There are three possible explanations for the observed decrease in electron intensity.

1) It is an instrumental effect caused by the modifications to the detector between 1965 and 1967.

2) It is a real change in the electron intensity incident at the top of the atmosphere

3) It is a combination of (1) and (2).

The relevant modifications made to the detector between 1965 and 1967 were the removal of a photomultiplier tube from the volume enclosed by the telescope and an increase of approximately 2.2 g cm^{-2} in the minimum amount of matter traversed by an electron before detection. These modifications counteract each other such that the 1967 detector should have a counting rate in the low energy component from 2-5% higher in 1967 than in 1965. This is the wrong order of magnitude to account for the observed intensity changes. We therefore conclude that we have observed modulation of the electron intensity in the energy region 30-600 MeV. The data enable a lower limit of 20% (low energy component) and 21% (high energy component) to be set on the modulation of electrons between 1965 and 1967.

Discussion

Recent results of experiments conducted above 5 g cm^{-2} of residual atmosphere are shown in Fig. 9. It should be noted that there is a decrease in the slope of the differential electron energy spectrum below an energy of

≈ 1 GeV. In this region our results are well represented by a spectrum of the form

$$\left(\frac{dJ}{dE}\right)_{150 < E < 800\ \mathrm{MeV}} = 14^{+2}_{-3}\ E^{-0.7\ \pm\ 0.1}\ /\mathrm{m}^2\ \mathrm{sec\ sr\ MeV}$$

where E is the electron energy in MeV and J is the electron intensity in particles/ m^2 sec sr. The differential spectrum is steeper both above 800 MeV and below 150 MeV. Our intensity is higher than those recently reported in a comparable energy range. However, balloon observations of primary electrons are inevitably susceptible to a significant correction for atmospheric secondary electrons. Discrepancies between results may reflect differences in interpretation of the size of the secondary component.

There is an interesting difference between the shape of the atmospheric depth versus intensity curves for electrons from flights made at Kiruna and Churchill Manitoba ($\lambda = 71°$N). It is noticed consistently for all energy intervals that the ratio, R, of the maximum intensity (at a depth ≈ 100 g cm^{-2}) to the intensity at 5 g cm^{-2} is larger for flights from Churchill than for flights from Kiruna. In Table V data are compared from Webber and Chotkowski (1967); L'Heureux (1967); Fanselow (1967) [Churchill] and from Bleeker et al (1967); present work [Kiruna]. This is clearly a possible source of disagreement over the primary intensity. This effect is present for all energy ranges above 20 MeV, and it is unlikely therefore, to be related to re-entrant albedo. The result is that a higher percentage of the measured intensity is claimed for primary origin at Kiruna than at Churchill. It should be noted that the atmospheric secondary electron intensity must be comparable at Churchill and Kiruna as it is derived from cosmic rays well above the classical Störmer cut-offs for both locations, or from gamma rays. Table V shows that the present result is in closest agreement with Webber and Chotkowski. The fact that results at Churchill differ from those at Kiruna must be regarded as coincidence; however, there may be serious differences in detector calibration which could account for the discrepancies in the depth curves. These discrepancies must not be ignored if balloon borne experiments are to provide meaningful data.

Jokipii, L'Heureux and Meyer (1967) have suggested, on the basis of a large diurnal variation, that a major percentage of the mid-day electron flux at Churchill is re-entrant albedo. They assume that the mid-day cut-off is enhanced, which increases the re-entrant albedo flux to account for an observed 100-200% increase in electron intensity in the energy region 20-270 MeV. These observations were from a series of balloon flights made in June and July both in 1965 and 1966. A diurnal variation in the electron flux has not been reported by Webber and Chotkowski (1967), Beedle and Webber (1967) or Fanselow (1967) who carried out flights from Churchill in July and August, 1965 and 1966.

It should not be ruled out that there is a seasonal variation in the cut-off at local noon. For example, at the summer solstice, at local noon, Churchill is approximately 36° from the Earth-Sun line in a plane normal to the ecliptic plane. In this position the interaction of the solar wind with the geomagnetic field may enhance the cut-off beyond expectation. However, at the winter solstice, at local noon, Churchill is 82° from the Earth-Sun line, and at this time the cut-off may be close to zero. Satellite results (Paulikas, Blake and Freden, 1968) suggest that high latitude cut-offs exhibit a complex temporal structure. The significance of geomagnetic longitude and geographic latitude in this context has yet to be understood. A noon enhancement of the cut-off may not be so marked at Kiruna in August, which could explain the absence of a diurnal variation in our results. On the other hand, at Churchill, in June, there may be a noticeable effect. At local noon in August Kiruna is approximately 48° from the Earth-Sun line.

There is no justification from our data for making a re-entrant albedo correction. A similar electron flux is observed both at noon and near midnight, apart from a slight increase which is attributed to increasing atmospheric depth and statistical effects. A possible mis-interpretation of the source of the noon flux would therefore not affect the midnight flux.

A decrease in the electron intensity is observed between 1965 and 1967 which appears to be independent of energy in the region 30-600 MeV (at the top of the atmosphere). The 1965 detector could not resolve electrons above 600 MeV and we are unable to compare results above this energy. Both in 1965 and 1967 no diurnal variation in the electron flux was observed, although the 1965 flight did not reach its floating altitude until 04.50 local time. There are two explanations for the decrease: a) the 1965 flight measured some re-entrant albedo which was not seen in 1967 and b) the change is caused by solar modulation. We feel the latter explanation is the more probable.

Results of O'Gallagher and Simpson (1967) suggest that solar modulation for protons is velocity dependent but rigidity independent below sound 1 GV (Gloeckler and Jokipii, 1967). The present result is consistent with a rigidity independent solar modulation of electrons below 600 MeV. The lower limit to the magnitude of the modulation is 20% between 30 and 600 MeV. This confirms the previous observation of solar modulation of high energy electrons by Webber and Chotkowski (1967).

Acknowledgements

The author wishes to thank his colleagues in the Cosmic Rays and Space Physics Group at Imperial College, London, for providing a stimulating environment, and particularly Professor H. Elliot for his interest and support. The Science Research Council provided financial assistance for the experimental programme. DESY, Hamburg and the Kiruna Geophysical Observatory respectively provided the accelerator and balloon launching facilities. Mr. K. E. Moss developed the pulse height analyser. We thank Dr. J. F. Ormes for his comments on the results.

References

Beedle, R. E. and W. R. Webber, Proc. 10th Int. Conf. Cosmic Rays (in press).

Bland, C. J., G. Boella, G. Degli Antoni, C. Dilworth, L. Scarsi, G. Sironi, B. Agrinier, Y. Koechlin, B. Parlier and J. Vasseur, Phys. Rev. Lett., 17, 813 1966.

Bleeker, J. A. M., J. J. Burger, A. J. M. Deerenberg, A. Scheepmaker, B. N. Swanenburg and Y. Tanaka, Proc. 10th Int. Conf. Cosmic Rays (in press).

Cline, T. L., G. H. Ludwig and F. B. McDonald, Phys. Rev. Lett, 13, 786, 1964.

Daniel, R. R. and S. A. Stephens, Phys. Rev. Lett. 15, 769 (1965).

Daniel, R. R. and S. A. Stephens, Phys. Rev. Lett, 17, 935 (1966).

Danjo, A., S. Hayakawa, F. Makino and Y. Tanaka, Proc. 10th Int. Conf. Cosmic Rays (in press).

Earl, J. A., Phys. Rev. Lett., 6, 125 (1961).

Fanselow, J. L., EFINS Preprint No. 67-76 (1967).

Freier, P. S. and C. J. Waddington, J. Geophys. Res. 70, 5753, (1965).

Gloeckler, G. and J. R. Jokipii, Ap. J. 148, 141 (1967).

Hakura, Y., J. Geophys. Res. 72, 1461, (1967).

Jokipii, J. R., J. L'Heureux and P. Meyer, J. Geophys. Res. 72, 4375 (1967).

L'Heureux, J., Ap. J. 148, 399 (1967).

L'Heureux, J. and P. Meyer, Phys. Rev. Lett. 15, 93 (1965).

L'Heureux, J. and P. Meyer, EFINS Preprint No. 67-52 (1967).

Meyer, P. and R. Vogt, Phys. Rev. Lett. 6, 193 (1961).

O'Gallagher, J. J. and J. A. Simpson, Ap. J. 147, 819, 1967).

Ormes, J. and W. R. Webber, Phys. Rev. Lett. 13, 106 (1964).

Paulikas, G. A., J. B. Blake and S. C. Freden, J. Geophys. Res. 73, 87 (1968).

Perola, G. C. and L. Scarsi, Nuovo Cimento, 46, 718 (1966).

Reid, G. C. and H. H. Sauer, J. Geophys. Res. 72, 4383 (1967).

Rossi, B., High Energy Particles, Prentice-Hall Inc. N.J. (1952).

Rubtsov, V. I., Proc 9th Int. Conf. Cosmic Rays (1966).

Schmoker, J. W. and J. A. Earl, Phys. Rev. 138, B, 300 (1965).

Simnett, G. M. London Univ. Thesis (1966).

Simnett, G. M. Plan. and Space Sc. 15, 1787, (1967).

Smorodin, Yu. A., Univ. of Chicago Publication, 1965).

Stone, E. C., J. Geophys. Res., 69, 3577 (1964).

Taylor, H. E., J. Geophys. Res. 72, 4467 (1967).

Verma, S. D., EFINS Preprint No. 66-44 (1966).

Webber, W. R. and C. Chotkowski, J. Geophys. Res. 72, 2783 (1967).

Figure Captions

Figure 1. Schematic cross section of the detector.

Figure 2. The vertical electron flux as a function of atmospheric depth for electrons which stop between 0 and 2 radiation lengths of lead (Group A). The depth dependences of the primary electron flux and the atmospheric secondary electron flux are indicated.

Figure 3. The vertical electron flux as a function of atmospheric depth for electrons which stop between 2 and 5 radiation lengths of lead (Group B). The depth dependences of the primary electron flux and the atmospheric secondary electron flux are indicated.

Figure 4. The vertical electron flux as a function of atmospheric depth for electrons which stop between 5 and 11 radiation lengths of lead. The flux is divided into groups C, D and E.

Figure 5. The vertical electron flux as a function of atmospheric depth for electrons which stop between 5 and 11 radiation lengths of lead (Groups C+D+E). The depth dependences of the primary electron flux and the atmospheric secondary electron flux are indicated.

Figure 6. The differential energy spectrum of atmospheric secondary electrons. Theoretical calculations by Perola and Scarsi (1966) and Verma (1966) for the solar minimum flux are shown for comparison.

Figure 7. The electron and "non electronic" counting rates as a function of time for August 6th, 1967.

Figure 8. The vertical electron flux as a function of atmospheric depth for electrons that stop between 0 and 5 radiation lengths of lead (low energy component) and between 5 and 11 radiation lengths of lead (high energy component) for 1965 and 1967.

Figure 9. The differential energy spectrum of primary cosmic ray electrons from recent measurements.

Table I

The Corrections Applied to the Raw Data

Particle	Total Correction Particles/cm^2 sec sr	% correction applied to each group					
		A	B	C	D	E	F
Proton	11 ± 1	15	30	15	20	10	10
α	0.9 ± 0.2		5	10	40	40	5
π meson	< 0.1						
μ meson	7 ± 2			100			
Z > 2	< 0.1						
Neutrons & γ rays	9 ± 2	20	20	20	20	15	5

Table II

Geographic and Geomagnetic Coordinates of the Balloon

at Different Times During the Flight

Time U.T.	Date	Geographic Latitude (°)	Geographic Longitude (°)	Geomagnetic Latitude (°)
21.38	5 Aug. 1967	67.8 N	20.2 E	65.3 N
23.36	5 Aug. 1967	68.7 N	20.2 E	66.1 N
10.54	6 Aug. 1967	69.3 N	16.1 E	67.3 N
14.00	6 Aug. 1967	69.9 N	14.0 E	68.2 N

Table III

The Peak Response of Each Electron Group

Electron Group	A	B	C	D	E	F
Electron energy for maximum response (MeV)	0	120	340	560	1100	1250

Table IV

The Flux of Primary Electrons. The Energies are Corrected to the Top of the Atmosphere

Electron Energy (MeV)	Flux Particles/m^2 sec sr
30 - 80	78
80 - 200	48
200 - 450	62
450 - 900	72
900 - 1500	40

Table V

The Ratio of the Electron Flux at 100 g cm^{-2} to the Electron Flux at 5 g cm^{-2}

(R) Measured by Different Experimenters at Churchill and Kiruna

Churchill			Kiruna		
Experimenter	Energy Interval (MeV)	R	Experimenter	Energy Interval (MeV)	R
Fanselow	42 - 76	10	Bleeker et al	200 - 360	1.8
	76 - 161	8		360 - 650	1.6
	161 - 430	9.5		650 - 1170	1.4
	430 - 840	4.6		>1170	<1
Webber & Chotkowski	60 - 180	6.6	Simnett	20 - 70	5.3
	180 - 360	4.6		70 - 190	5.0
	360 - 750	4.0		190 - 440	3.6
	>750	2.0			
L'Heureux	10 - 230	8			
	230 - 400	10			
	400 - 710	10			
	710 - 4900	2.0			

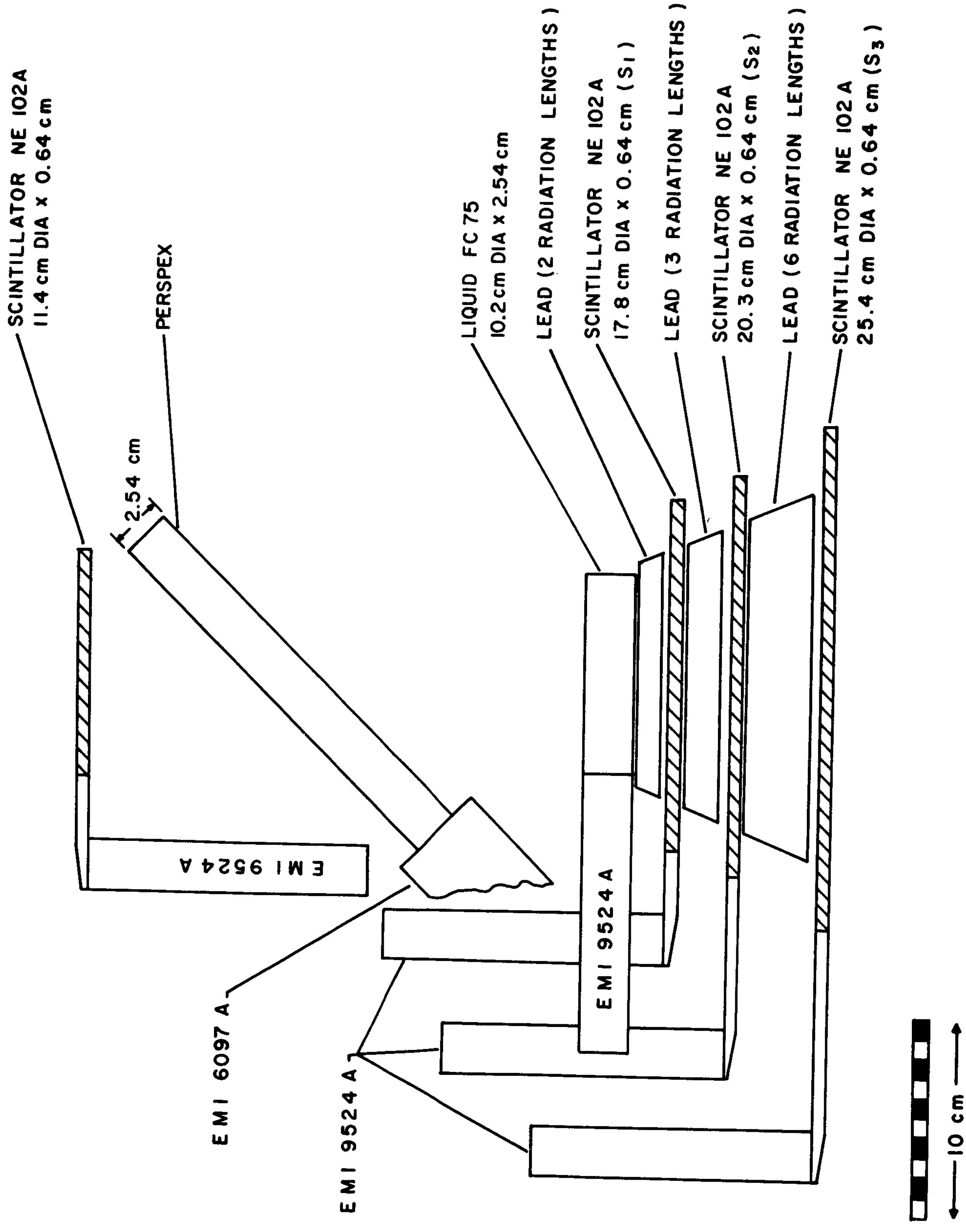
SCINTILLATOR NE 102A
11.4 cm DIA x 0.64 cm
PERSPEX
2.54 cm
LIQUID FC 75
10.2 cm DIA x 2.54 cm
LEAD (2 RADIATION LENGTHS)
SCINTILLATOR NE 102A
17.8 cm DIA x 0.64 cm (S_1)
LEAD (3 RADIATION LENGTHS)
SCINTILLATOR NE 102A
20.3 cm DIA x 0.64 cm (S_2)
LEAD (6 RADIATION LENGTHS)
SCINTILLATOR NE 102A
25.4 cm DIA x 0.64 cm (S_3)
EMI 9524 A
EMI 9524 A
EMI 6097 A
EMI 9524 A
10 cm

Figure 1

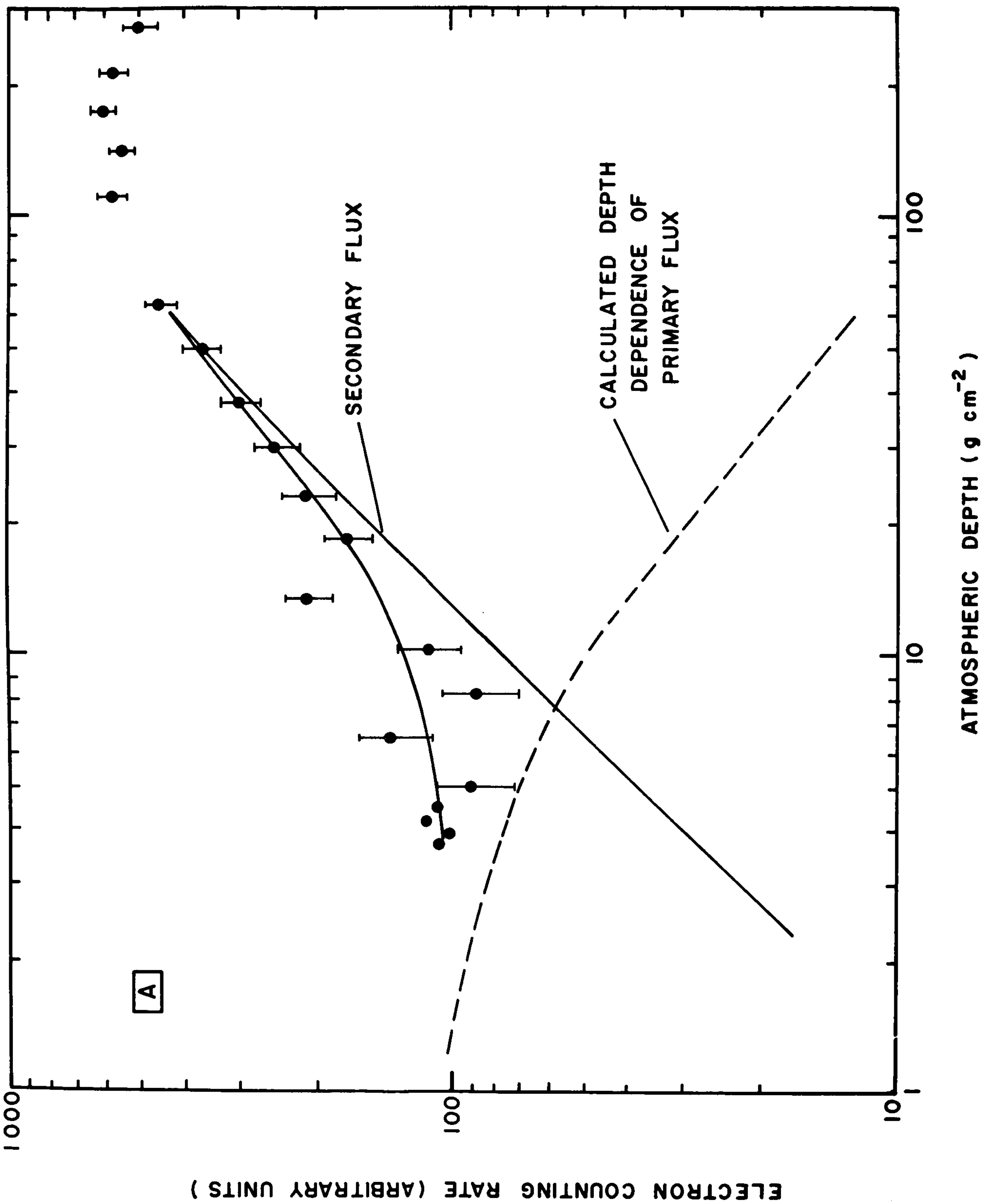
A
SECONDARY FLUX
CALCULATED DEPTH
DEPENDENCE OF
PRIMARY FLUX
ATMOSPHERIC DEPTH (g cm^{-2})
ELECTRON COUNTING RATE (ARBITRARY UNITS)
1000
100
10

Figure 2

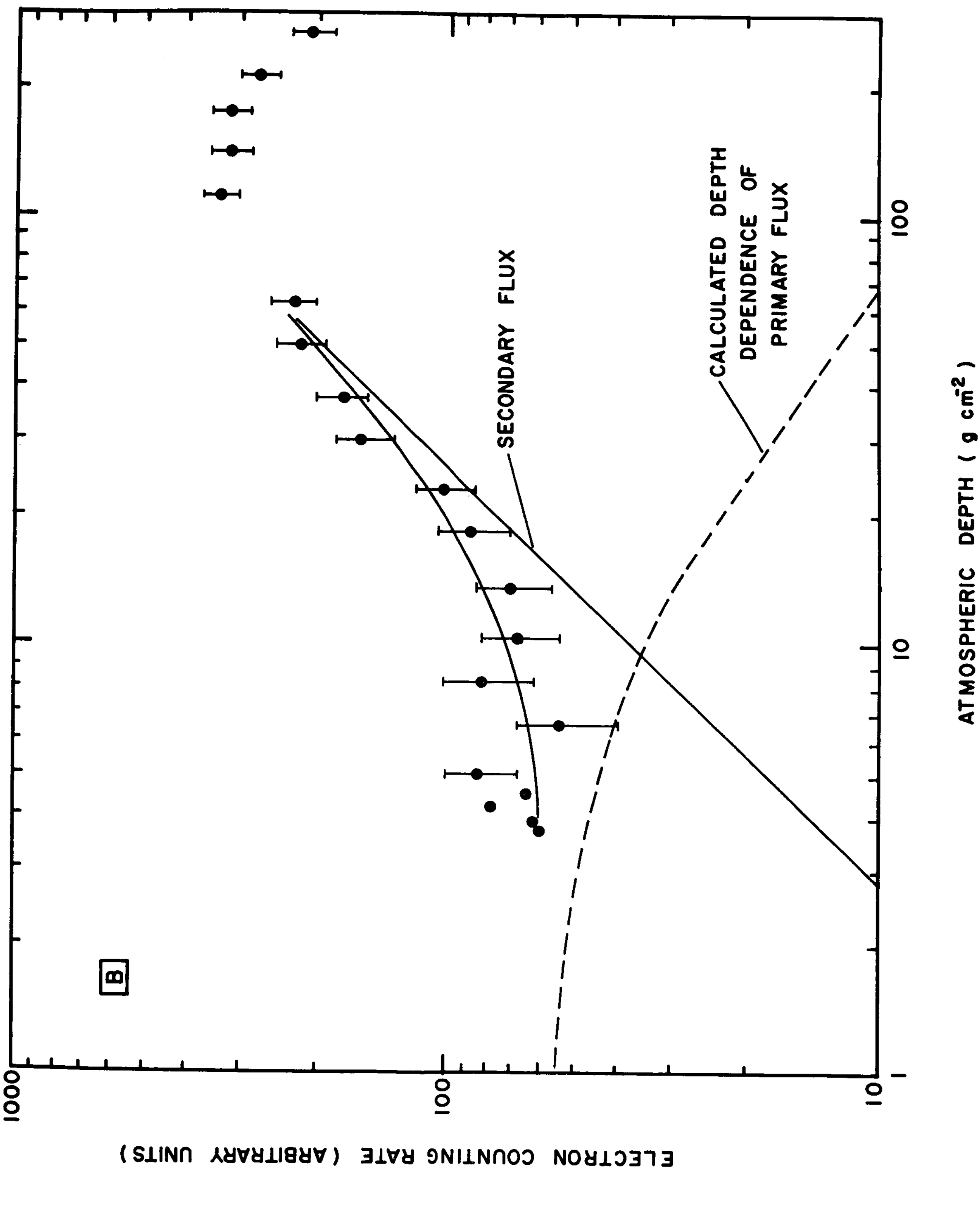
B
SECONDARY FLUX
CALCULATED DEPTH DEPENDENCE OF PRIMARY FLUX
ATMOSPHERIC DEPTH (g cm^{-2})
10
100
ELECTRON COUNTING RATE (ARBITRARY UNITS)
1000
100
10

Figure 3

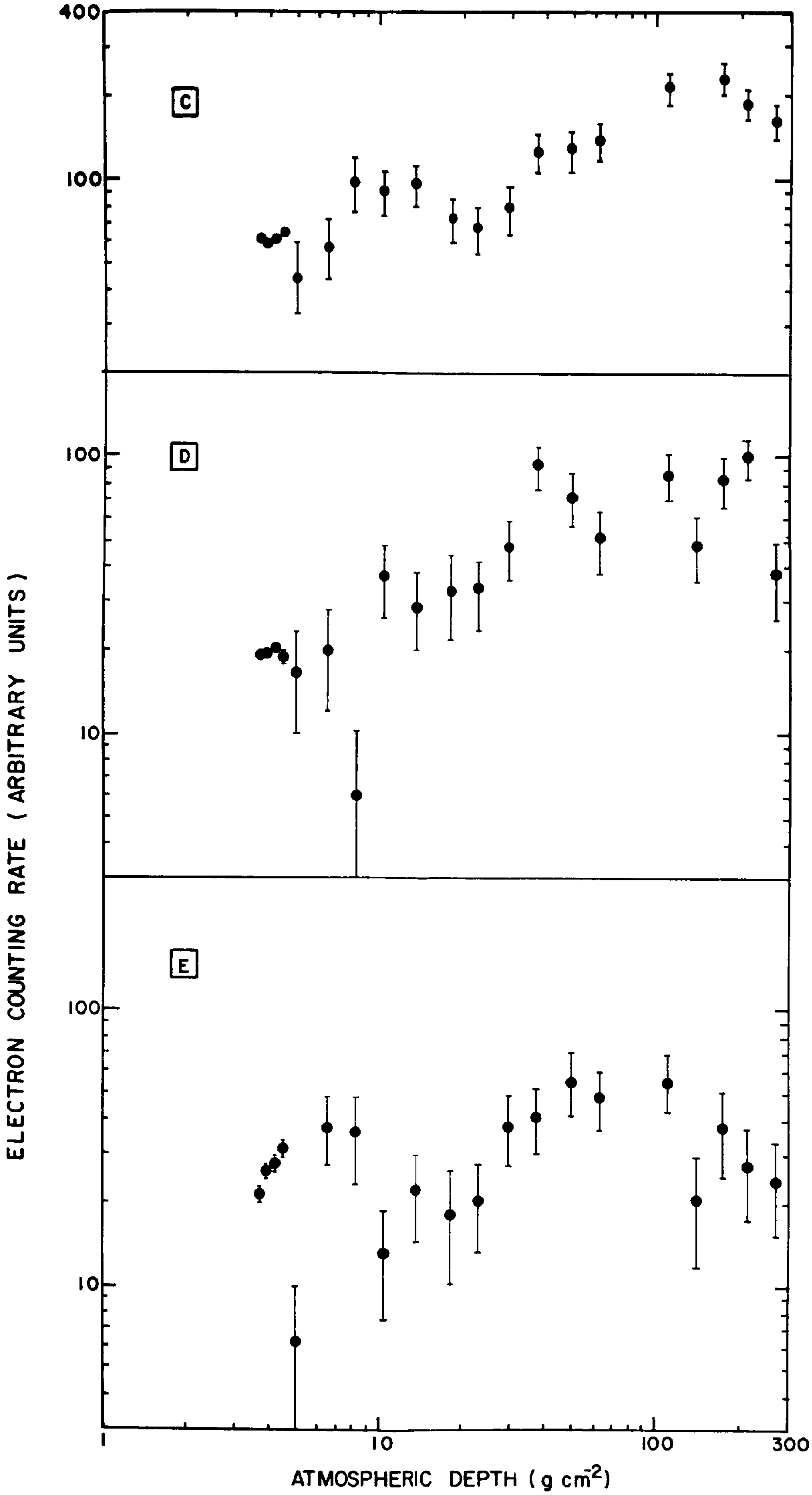

C
D
E
400
100
10
1
10
100
300
ELECTRON COUNTING RATE (ARBITRARY UNITS)
ATMOSPHERIC DEPTH (g cm^{-2})

Figure 4

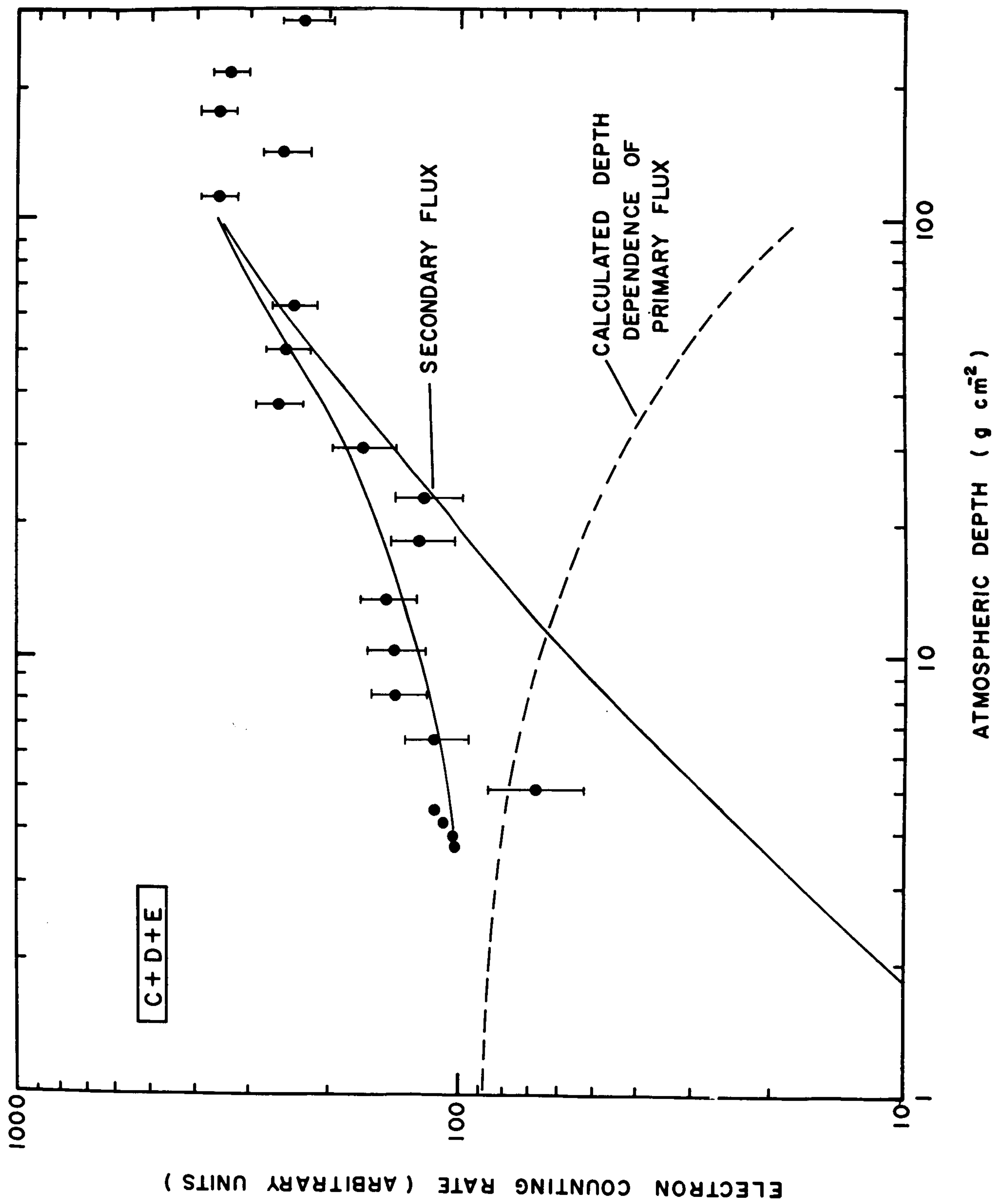
C+D+E
SECONDARY FLUX
CALCULATED DEPTH DEPENDENCE OF PRIMARY FLUX
ATMOSPHERIC DEPTH (g cm^{-2})
ELECTRON COUNTING RATE (ARBITRARY UNITS)
1000
100
10
1
10
100

Figure 5

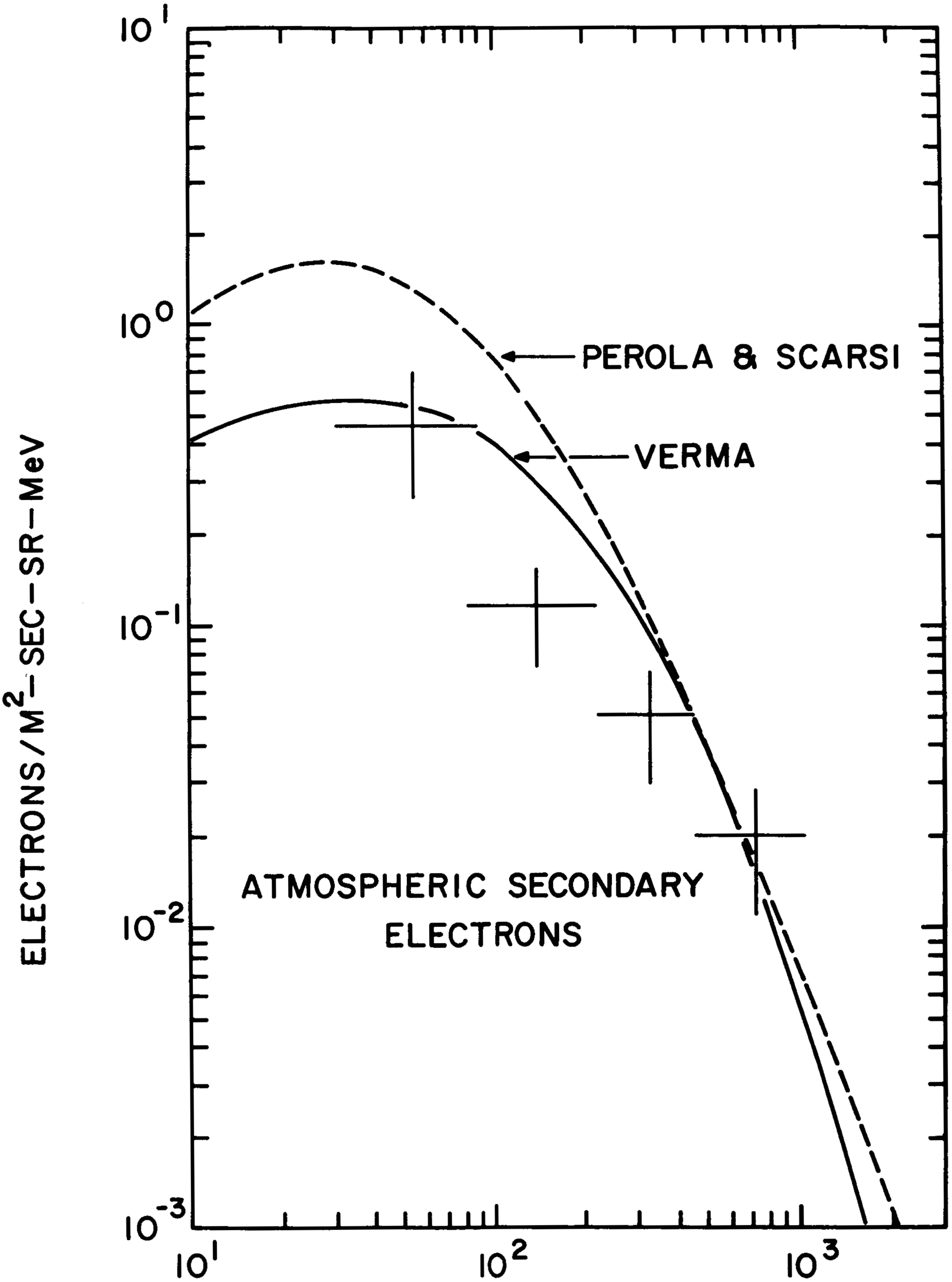

10^1
10^0
10^{-1}
10^{-2}
10^{-3}
ELECTRONS/M^2-SEC-SR-MeV
PEROLA & SCARSI
VERMA
ATMOSPHERIC SECONDARY ELECTRONS
10^1
10^2
10^3
ELECTRON ENERGY (MeV)

Figure 6

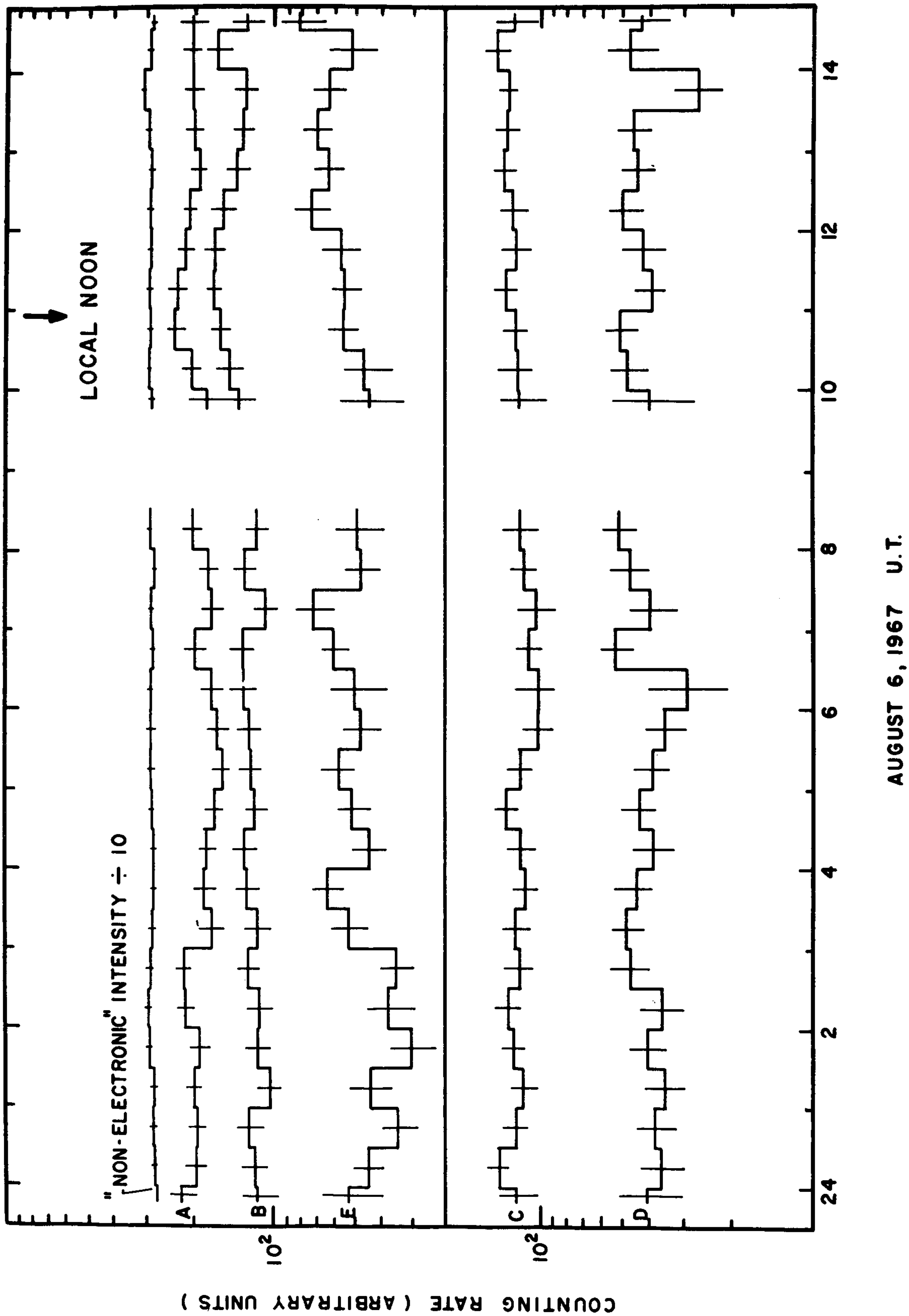

"NON-ELECTRONIC" INTENSITY ÷ 10
LOCAL NOON
A
B
E
C
D
10^2
10^2
24
2
4
6
8
10
12
14
AUGUST 6, 1967 U.T.
COUNTING RATE (ARBITRARY UNITS)

Figure 7

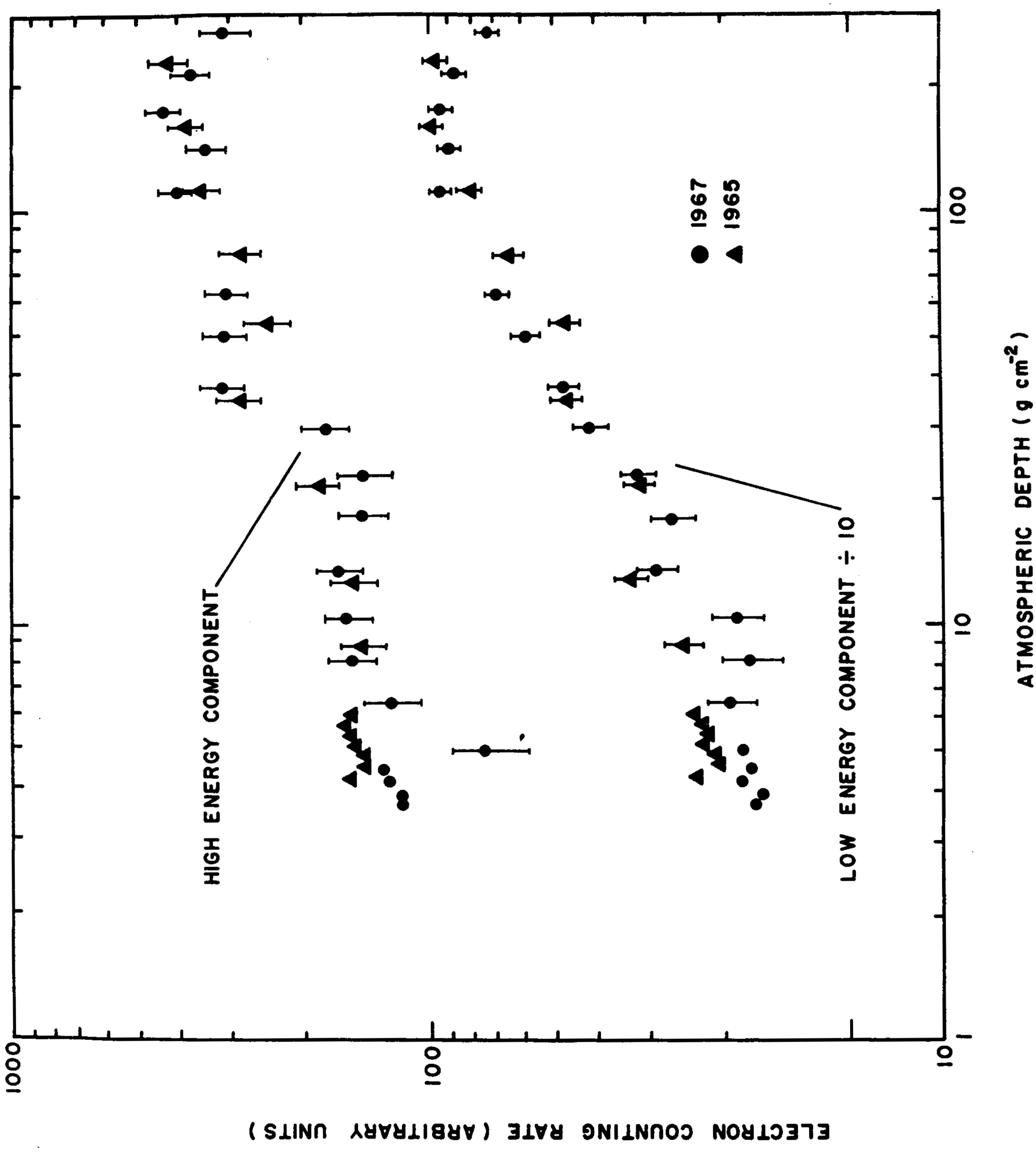

HIGH ENERGY COMPONENT
LOW ENERGY COMPONENT ÷ 10
1967
1965
ATMOSPHERIC DEPTH (g cm^{-2})
ELECTRON COUNTING RATE (ARBITRARY UNITS)
1000
100
10
1
10
100

Figure 8

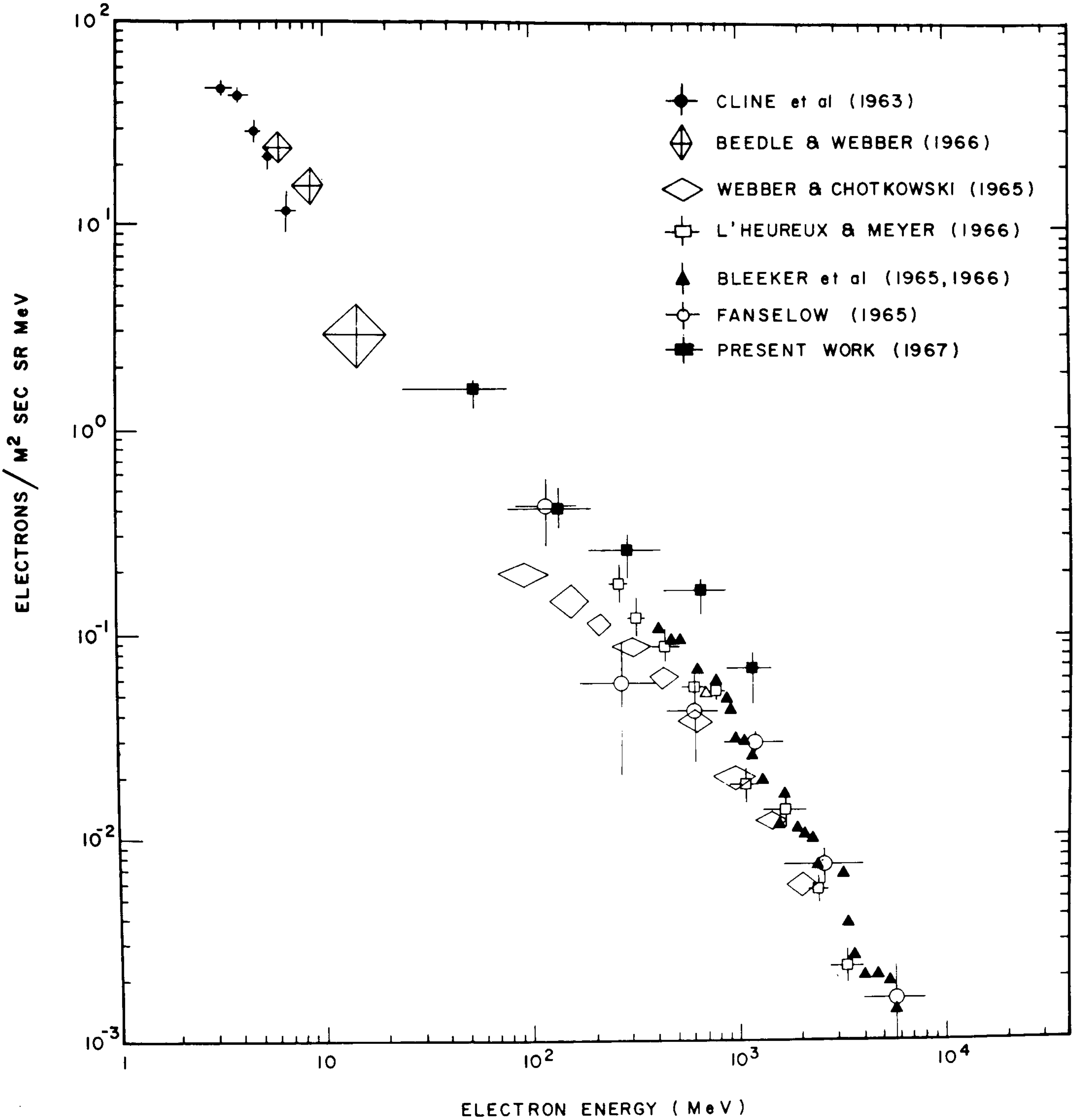

CLINE et al (1963)
BEEDLE & WEBBER (1966)
WEBBER & CHOTKOWSKI (1965)
L'HEUREUX & MEYER (1966)
BLEEKER et al (1965, 1966)
FANSELOW (1965)
PRESENT WORK (1967)
ELECTRONS/M² SEC SR MeV
ELECTRON ENERGY (MeV)

Figure 9